---

**Article:**
Tse, C., Whiteley, R., Yu, T. et al. (4 more authors) (2016) Inkjet printing Schwann cells and neuronal analogue NG108-15 cells. Biofabrication, 8 (1). 015017. ISSN 1758-5082

https://doi.org/10.1088/1758-5090/8/1/015017

---

# Inkjet printing Schwann cells and neuronal analogue NG108-15 cells

**Christopher Tse[1], Robert Whiteley[1], Tong Yu[2], Jonathan Stringer[1], Sheila MacNeil[2], John W. Haycock[2] and Patrick J. Smith[1]**

[1]Department of Mechanical Engineering, Laboratory of Applied Inkjet Printing, D 03, Royal Exchange Manufacturing Building, 64 Garden Street, Sheffield, S1 4BJ, UK; telephone: +44(0)144-222-7738, fax: +44(0)114-222-7890; e-mail: Patrick.Smith@sheffield.ac.uk

[2]Department of Materials Science & Engineering, Kroto Research Institute, University of Sheffield, North Campus, Broad Lane, Sheffield, S3 7HQ, UK

E-mail: mtp11cct@sheffield.ac.uk and Patrick.smith@sheffield.ac.uk

**Abstract**

Porcine Schwann cells and neuronal analogue NG108-15 cells were printed using a piezoelectric-inkjet-printer within the range of 70V to 230V, with analysis of viability and quality after printing. Neuronal and glial cell viabilities of >86% and >90% were detected immediately after printing and no correlation between voltage applied and cell viability could be seen. Printed neuronal cells were shown to produce neurites earlier compared to controls, and over several days, produced longer neurites which become most evident by day 7. The number of neurites becomes similar by day 7 also, and cells proliferate with a similar viability to that of non-printed cells (controls). This method of inkjet printing cells provides a technical platform for investigating neuron-glial cell interactions with no significant difference to cell viability than standard cell seeding. Such techniques can be utilized for lab-on-a-chip technologies and to create printed neural networks for neuroscience applications.

Keywords: Inkjet printing, cell printing, nerve printing, tissue engineering

Submitted to Biofabrication

## 1. Introduction

Conventional methods of tissue engineering involve manually seeding cells onto scaffolds (Langer & Vacanti 1993). However, cell printing has potential for applications in tissue engineering (Xu, Zhao,

Zhu, Mohammad Z Albanna, et al. 2013; Zhang et al. 2012). The ability of inkjet printing to combine a high-throughput deposition capability with high precision placement of biomaterials (Wilson & Boland 2003; Boland et al. 2003) allows it to be employed for in vitro tissue engineered models, especially if one can print eukaryotic cells which are undamaged and able to proliferate and differentiate as required post printing.

Saunders (et al. 2008) reported on the ability to print human HT1080 fibrosarcoma cell suspensions using a drop-on-demand piezoelectric system and found that viability after printing reached 98%, compared to controls. Similarly, Boland et al reported on thermal drop-on-demand printing to print Chinese Hamster Ovary (CHO) cell suspensions, and found that cell viability was >90% after printing (Xu et al. 2005). The findings of Boland and others indicate that adherent eukaryotic cells can be delivered by inkjet printing without substantial damage. Embryonic neuronal cells (including hippocampal, cortical and motor neurones), stem cells, muscle cells and chondrocytes have all been inkjet printed with resultant survival and growth (Xu, Zhao, Zhu, Mohammad Z. Albanna, et al. 2013; Cui et al. 2010; Lorber et al. 2013; Cui et al. 2012; Ilkhanizadeh et al. 2007; Phillippi et al. 2008). This accumulating research brings us closer to a viable strategy for in vitro 3D lab devices and to treating damage to the nervous system (Schmidt & Leach 2003; Ma et al. 2004).

The ability to deposit cells at predefined positions over a relatively short period of time allows better experimental design for the study of intercellular interactions. Accurate positioning of cells can lead to the creation of spatially dependant cell-containing devices to promote the advancement of tissue engineered constructs and the creation of fine neuronal networks (Schwarz et al. 2014; Tomba et al. 2014). This can also help with the understanding of how cells behave in relation to the topography of the substrate (Discher et al. 2005). Ongoing research in the field of bioengineering with inkjet printing aims at creating tissues with multiple cell types within a scaffold for mimicking native tissue, which is a progressive step towards organ printing. The ability to create tailored tissues quickly and reproducibly will offer scientists a very powerful tool in regenerative medicine and in vitro research. Researchers have successfully created small sections of tissue through additive manufacturing

techniques for drug testing and toxicology (Miller et al. 2012; Inamdar & Borenstein 2011; Wang et al. 2007), with more complex cell combinations to be created in the near future.

Neuronal cells are surrounded by glial (or Schwann) cells in the peripheral nervous system and the co-interaction between them and their surrounding environment are essential for nerve function. A current challenge in peripheral nervous system injury is to find an alternative to autologous nerve grafting.

This study describes a method for inkjet printing NG108-15 neuronal cells and Schwann cells with phenotypic analysis over 7 days, with cell viability assessed immediately and 7 days post printing, and the extent of neurite outgrowth of printed neuronal cells was also assessed. Printing of fibroblasts was included for comparison. In previous studies inkjet printing of neurons and their viability was reported (Xu et al. 2005; Lorber et al. 2013), but a maximum of 80V was used. The current study expands the printing parameters to 230V, and describes a more detailed phenotypic analysis of Schwann cells.

To the best of our knowledge, the use of piezoelectric inkjet printing to organize neuronal and Schwann cells has not been reported previously using such a broad range of voltages. The outcome of this work provides a broad platform for developing IJP nerve constructs e.g. for 3D in vitro devices, nerve regeneration approaches or the study of neurodegenerative diseases.

## 2. Materials and Methods

### 2.1. Inkjet Printing System

A single 60 µm nozzle piezoelectric inkjet device (MicroFab, Texas, USA) was used to print each cell type (Figure.1). Specifically, this was a Jetlab 4 xl-A tabletop-printing platform with positional accuracy and repeatability of 25 µm and 5 µm, respectively, equipped with drop-on-demand PH-46 print heads (MicroFab, Texas, USA). Independent polypropylene fluid reservoirs kept the printing inks isolated prior to jetting, and the dispensing devices were connected together through PTFE fittings and tubings. A CT-PT4 four channel pressure controller was used (MicroFab, Texas, USA) to

maintain a slight negative pressure within the system to control a nozzle meniscus level for optimal jetting. A JetDrive III was used to control the generation of a waveform and tailor the jetting parameters to the print heads.

Prior to jetting, all tubing, reservoirs and print heads were flushed with 1% (v/v) Micro-90 cleaning solution (10mL for 10 minutes), distilled de-ionised water (20mL for 30 minutes) and subsequently with cell culture medium (DMEM / 10% fetal calf serum (FCS)). Unless otherwise stated, the inkjet printer was calibrated to print at 2 kHz, 80V, rise time 36µs, dwell time 42µs, fall time 50µs and printed within 3mm from the ~~surface of the substrate~~substrate and nozzle. Viability experiments used voltages from 70V with increasing increments of 20V to a maximum of 230V. This setup proved most stable for producing droplets. All samples were jetted into 12 well flat bottom cell culture plates (Costar) at room temperature. Approximately 300 µL was jetted into each well at a concentration of $2x10^5$ cells/mL with their respected variables. Inkjet printing was performed within 30 minutes of loading a cell suspension into the print reservoir. It was established from initial work that both fibroblasts and neuronal cells could be printed for up to 40 minutes without significant loss of cell


Figure 1. Photograph showing the Microfab piezoelectric printer used for this study, with magnified images of the CCD camera, printhead holding platform, and print head during jetting.

number.

2.2. Human dermal fibroblast cells, NG108-15 neuronal cells and Schwann cells

Human dermal fibroblasts were obtained from abdominoplasty or breast reduction operations according to local ethically approved guidelines (under an HTA Research Tissue Bank license number 12179), and were used as controls to compare viability of the different cell types. NG108-15 neuronal cells were obtained from the European Collection of Cell Cultures (ECACC Health Protection Agency Culture Collections, Porton Down, UK). Primary porcine Schwann cells were isolated from both tibial and fibular nerve tissue under the Animal (Scientific Procedures) Act 1986. These were cultured in a humidified 37°C/5% $CO_2$/95% air (v/v) environment in Dulbecco's modified Eagle's medium (DMEM; Sigma) containing 10% (v/v) FCS (Gibco, UK), 1% (v/v) L-glutamine (Gibco, UK), 1% (v/v) penicillin/streptomycin (Gibco, UK), and 0.5% (w/v) amphotericin B (Gibco, UK). Porcine Schwann cells had 0.150% (v/v) bovine pituitary extract (BPE) (Sigma, UK) and 0.02% (v/v) forskolin (Sigma, UK) added to their cell media. Cells were cultured in a humidified 37°C/5% $CO_2$/95% air (v/v) environment. FCS was removed from the medium on neuronal cells to induce cell differentiation and neurite formation when optimal cell density was achieved. Prior to seeding, cells were grown to confluence, and detached with 0.05% (w/v) trypsin/EDTA (GIBCO, Invitrogen, Karlsruhe, Germany). A Neubauer chamber was used to count cells and passages 9 to 12, 16 to 19 and 2 to 3 were used for experimentation respectively.

2.3. Well plate modification for Schwann cell culture after Inkjet Printing

Previous experiments showed Poly-L-lysine and fibronectin to support Schwann cell growth (Daud et al. 2012; Baron-Van Evercooren et al. 1982), and therefore these were implemented within this paper. The 12-well plates were coated with 0.5mg/mL poly-L-lysine and 0.5mg/mL fibronectin respectively for 10 minutes at room temperature on a platform rocker (STR6, Bibby Stuart). After discarding the used poly-L-Lysine and fibronectin, the well plates were dried at room temperature for 2 hours before being washed with warm PBS twice. TCP 12-well plates were used as controls.

2.4. Trypan blue staining for cell viability immediately after inkjet printing

Cell suspensions were mixed and stained with equal volumes of Trypan blue and analysed visually by bright field light microscopy. Cells staining positive for blue dye uptake indicated loss of membrane integrity and were counted as dead (or damaged). In contrast, cells excluding Trypan blue dye appearing bright coloured were counted as live. A live/dead percentage was calculated to give population cell viability immediately after inkjet printing. 30 randomly selected microscope fields of view per experimental condition were selected.

2.5. MTT metabolic activity for assessing cell viability 1, 3 and 7 days post printing

To investigate the longer term effects of inkjet printing on cells, samples were analysed for metabolic viability by MTT (3, 4, 5-dimethylthiazol-2,5-diphenyl tetrazolium bromide) assay at each time point. Fibroblasts and NG108 neuronal cells were cultured on TCP, and Schwann cells were cultured on TCP, poly-L-lysine and fibronectin. Non-printed cells were used as a reference control. After deposition, cells were re-suspended at a density of $4x10^4$/mL and seeded into a 24 well plate in triplicate. Culture medium was removed and the samples were gently washed with PBS x1 and 1mL of 0.5mg/mL MTT (in PBS) solution was added. The rate of formazan crystal formation through MTT reduction is proportional to the metabolic activity of the cells. After incubation for 90 minutes at 37°C, unreacted MTT solution was aspirated and replaced with 200 µL acidified isopropanol (0.1% (v/v) HCl in isopropanol), dissolving the purple crystals. 200 µL of solution was then transferred into 96-well plates, and read in a BIO-TEK ELx 800 microplate reader at 540nm and referenced at 630nm.

2.6. Neurite analysis of NG108-15 neuronal cells 1, 3 and 7 days after inkjet printing

Neuronal cells were prepared as described above, but cultured in DMEM without fetal calf serum, to stimulate neuronal differentiation (Seidman et al. 1996). These are reported to be morphologically different to cells cultured with serum (Kowtha et al. 1993). Images were obtained using an inverted Olympus CK40 phase contrast microscope. 5 images were sampled from randomly selected fields of view. 10 cells were analysed in each image from the top left corner. This approach was followed consistently to prevent bias. This gave a total of 50 cells being analysed for each measured variable.

Morphological characterisation techniques employed were adapted from previously published work (Daud et al. 2012). Cells were only analysed if their cell body was not touching another cell and if the whole of the cell, including neurites, was visible in the image and the neurite length was measured. A process twice as long as the length of the cell body was counted as a neurite. The number of neurites per neuronal cell was quantified, together with the percentage of neuronal cells bearing neurites.

2.7. S-*100β and DAPI* immunolabelling for identification of Schwann cells

Immunolabelling of S-100β protein was used to determine the overall purity of the cell culture on different well surfaces. Cells were labelled on days 1, 3 and 7. At each time point, Schwann cell growth medium was discarded and cells washed 3 times with PBS (5 min each wash). 500 μL per well of 3.7% (vol/vol) formaldehyde solution was added for 20 min at 4 C to fix Schwann cells and then washed with PBS (3×5 min). Cells were permeabilized with 500 μL of 0.1% (vol/vol) Triton-X100 for 20 min at room temperature and washed three times with PBS for 5 min. At room temperature, 500 μL of 7.5% BSA per well was added and incubated at room temperature for 60 min, followed by 1% BSA wash once. Primary antibody (rabbit polyclonal anti-S100β antibody (1:250)) (Dako, Denmark) was prepared in 1% BSA and incubated with the samples at 4°C overnight. Primary antibody was removed and followed by 3x PBS washes (10 min each). Samples were then incubated with goat anti-rabbit IgG H&L FITC secondary antibody (1:100 in 1% (vol/vol) BSA) (Vector Labs, USA) at room temperature in the dark for 1 h.

0.1% (vol/vol) DAPI (Sigma Aldrich) was diluted in PBS and added in the samples in the absence of light and at room temperature, after removing secondary antibody, and washed three times (5 min each) with PBS. PBS was left on the samples to avoid samples drying. After immunolabelling, samples were stored at 4°C in the dark before conducting confocal microscopy.

Samples were imaged using an inverted Zeiss LSM 510 META confocal microscope, using an argon 30mW ion laser (488nm) for FITC excitation λex = 495 nm / λem = 521 nm. Nuclei were visualized by two photon excitation using a Chameleon Ti-Sapphire tuneable laser λex = 800 nm / λem = 461 nm. 5 images were sampled from randomly selected fields of view and Schwann cells were identified

if DAPI labelled nuclei were co-labelled with an S-100β positively labelled cytoplasm. Cells were counted and a percentage of positively labelled Schwann cells were compared to the whole sample population.

## 3. Results and Discussion

### 3.1. Cell viability of fibroblasts, NG108 neuronal cells and Schwann cells immediately after inkjet printing

Figure 2 shows the effect of inkjet printing voltage on the viability of human dermal fibroblasts, NG108-15 neuronal cells and primary porcine Schwann cells assessed by Trypan blue staining. Fibroblast cells were printed as another form of control, and as a reference to previously published work (Saunders et al. 2008).

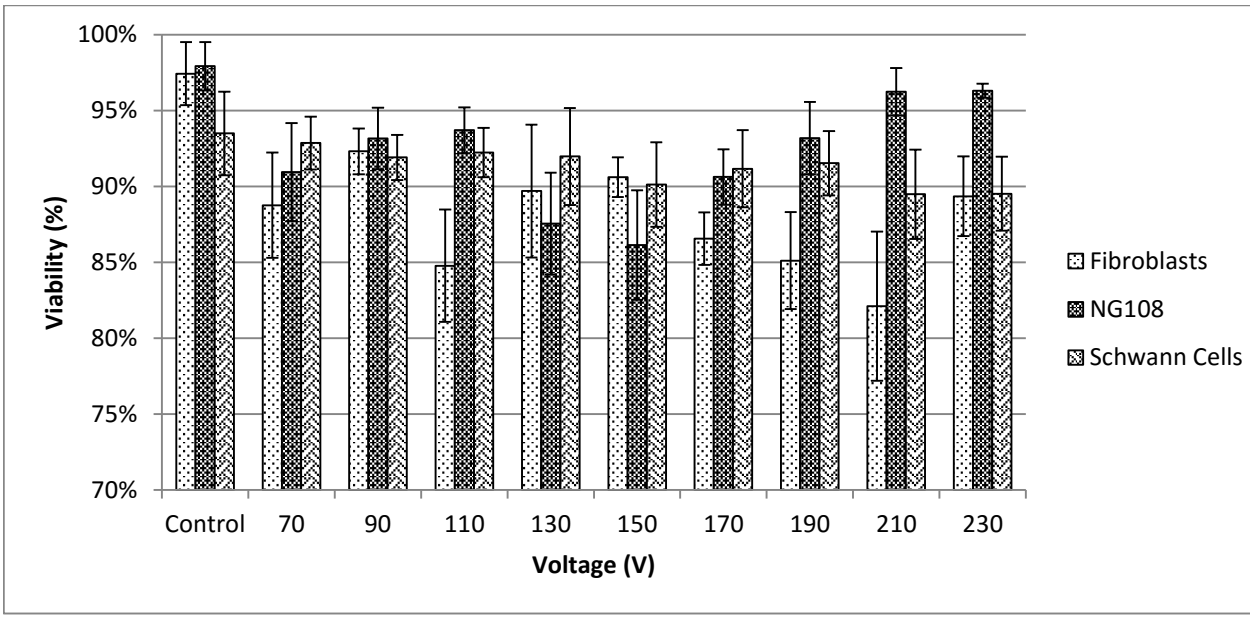


Figure 2. Analysis of mean viability of cells assessed using trypan blue staining immediately after inkjet printing, with standard deviation error bars at different voltages with each cell type. Cells were printed at a frequency of 2kHz. N=30.

Non-printed control samples showed cell viability of >90%. Inkjet printing resulted in a cell viability of 82-92% for fibroblasts, 86-96% for neuronal cells and 89-92% for Schwann cells. There was no correlation between the range of voltages used (between 70-230 V) and cell viability. It was hypothesised that an increase in voltage would increase the shear stress to the cells passing through the glass nozzle of the print head. However, the use of this range of forces did not show a

proportionate amount of damage to the cells. It may be that this is due to the cell culture medium (which contains 10% foetal calf serum) behaving to buffer the physical shock between the cell and the interior of the print head, thus decreasing the friction experienced by cells. The viability determined was comparable with that reported previously for fibroblasts (Saunders et al. 2008), where an HT1080 fibroblast cell line had 94% viability when printed at 80V. Fibroblasts used in the present study were human primary cells, in contrast to that of Saunders (et al 2008).

The viability of neuronal cells, glial cells and fibroblasts were similar with no significant differences in metabolic activity identified between the cell types at any of the voltages studied compared with non-printed control cells. It is important to note that the applied voltage causes the actuation of the piezoelectric crystal and hence, under the optimum parameters, will eject a droplet out of the nozzle. The voltage applied to the print head does not come into direct contact with the cell culture medium and is therefore not subject to direct conductive electron transfer. An increase in voltage causes a stronger piezoelectric response and cells in the culture medium are ejected with more force through a narrow orifice. The velocity that droplets travelled was calculated between 3.2 – 13.1 $ms^{-1}$ at 70 – 230 V, and corresponded to a shear rate of 5 x $10^4$ – 2 x $10^5$ $s^{-1}$ respectively.

Over time, cells will begin to aggregate within the printing system and eventually clog the print head, stopping further inkjet printing. Parsa (et al. 2010) used biocompatible surfactants e.g. Pluronic in combination with physical agitation (stirring) to alleviate restrictions in printing time and maintain cell printing consistency, delaying cell sedimentation and overall increased reliability in the process. Our own studies showed cell printing produced viable cells up to a maximum of 40 minutes after loading into the inkjet printer without the need for surfactants or stirring. This finding is in line with previous studies that report a 20 to 40 minute cell deposition time is possible before cell aggregation (Lorber et al. 2013; Pepper et al. 2011; Saunders et al. 2008). Such studies showed a decrease in cell number after 40 minutes and it was speculated that this was caused by sedimentation of cells to the bottom of the print reservoir and also through adherence to the tubing and glass capillary of the print head. Both were confirmed independently, through a clear visual indication over time of a layer of

cells being formed at the bottom of the polypropylene reservoir, and cells could be flushed out from the printing head by the addition of trypsin at the end of a print experiment.

### 3.2. Schwann and NG108 neuronal cell proliferation 1, 3 and 7 days after inkjet printing

Schwann cell concentration on different surface coatings after printing was assessed. As shown in Figure 3 all cell types showed an increase in metabolic activity through MTT analysis, with the largest differences arising between days 3 and 7.

There was a suggestion that Schwann cells proliferated slightly better on fibronectin-coated tissue culture plastic (TCP). Fibronectin is an extracellular glycoprotein involved in wound healing and remylination for functional nerve regeneration (Ahmed & Brown 1999; Akassoglou et al. 2002) and our studies confirmed fibronectin as the best culture surface compared to TCP or poly-L-lysine for Schwann cells, as identified by viability and S-100β immunolabelling (to confirm purity). The largest difference observed was at day 7, which showed that inkjet printed cells, and cells cultured on fibronectin, had a higher viability versus control, and consequently had a higher cell number at this time after printing. This research supports previous findings that fibronectin is a better culturing environment that TCP and Poly-L-Lysine (Daud et al. 2012)

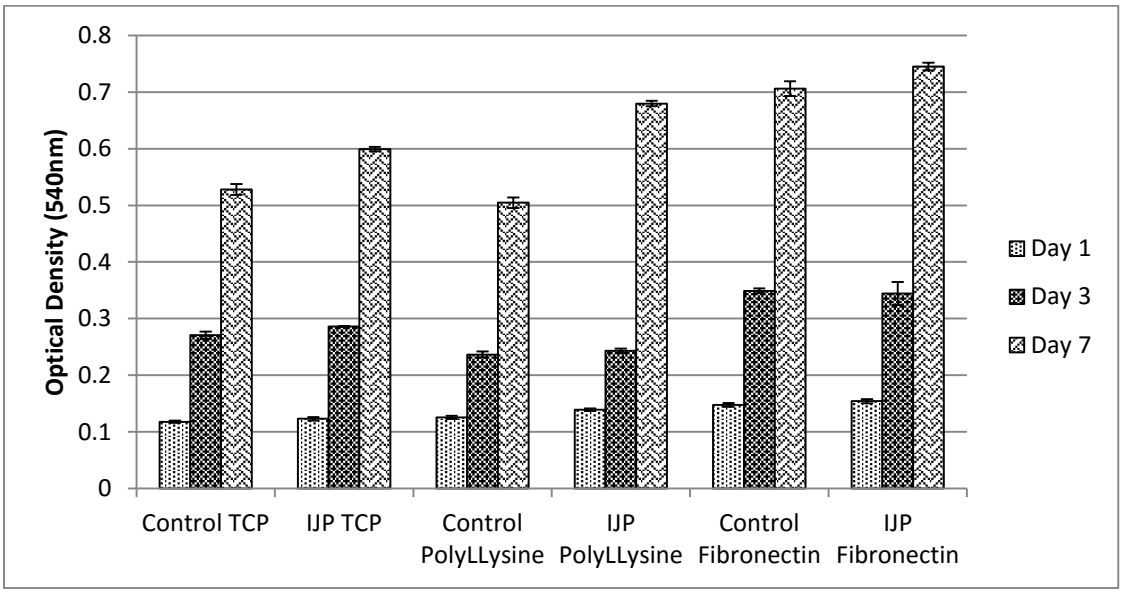


Figure 3. MTT assay results of Schwann cells ~~printed and non-printed Schwann cells~~ after 1, 3 and 7 days on different substrate surfaces, with standard deviation. Inkjet printed (IJP) cells were printed at 80V and 2kHz. N=3

NG108-15 neuronal cells were inkjet printed and had very similar viabilities to control samples, increasing exponentially over time (Figure 4). By day 7, using light microscopy and viability measurement, cells were shown to be confluent and no difference was observed between control and printed cells.

If inkjet printing had a significant detrimental effect on cells, a decrease in cell number would be seen compared to controls over time from which the cells might not recover. However this was not seen and the cells were comparable to control samples. This finding is of interest as it confirms that inkjet printing does not affect cell viability or growth over 7 days post printing. This is encouraging as it supports the development of this technique for applications such as tissue engineered constructs and 3D models.

When comparing the optical density readings of Schwann cells (Figure 3) with NG108 neuronal cells (Figure 4), it is clear that neuronal cells have a higher metabolic activity than Schwann cells. This is due to the nature of cell lines having a higher metabolic activity than primary cells, which both have very different growth rates due to their differences in function and origin.

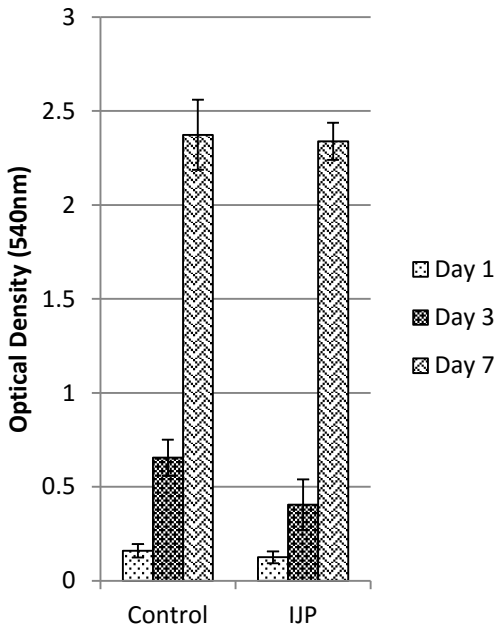


Figure 4. MTT assay results of NG108-15 neuronal cells when grown with serum in media after inkjet printing at 80V and 2kHz, with standard deviation. N=3

### 3.3. Schwann cell purity after inkjet printing

S100β immunolabelling was assessed to determine Schwann cell purity after IJP on different substrates (Figure 5). Schwann cells positively immunolabelled with FITC and DAPI, whilst fibroblasts (which can potentially contaminate cultures from the isolation procedure) stain only with DAPI. All cells were identified as Schwann cells irrespective of being inkjet printed or not on the different substrates and this therefore confirms that Schwann cells maintain their purity, and grow at the same rate as control samples after inkjet printing.

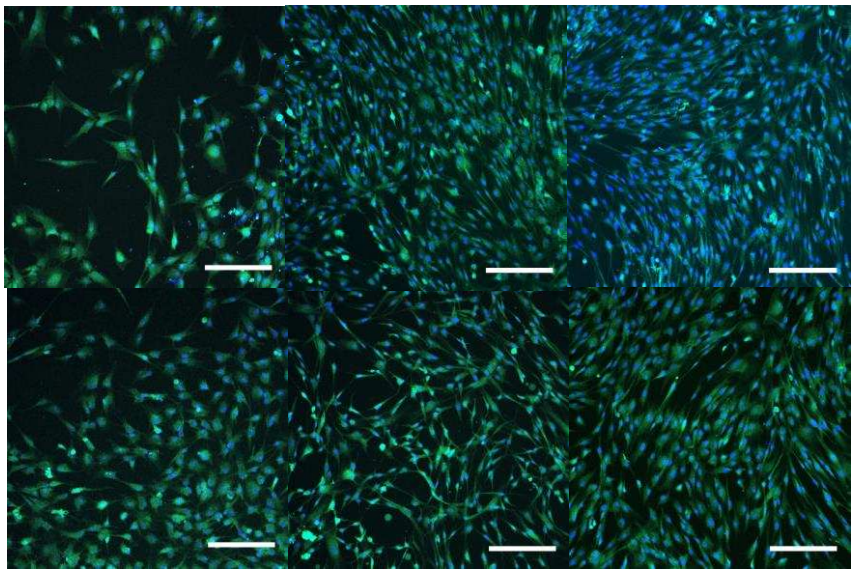

Figure. 5. Confocal micrograph images showing Schwann cells stained for actin (green; S100β) and nuclei (blue; DAPI). Top micrographs show inkjet printed Schwann cells at 80V and 2kHz after 1, 3 and 7 days respectively. Bottom micrographs show control samples without inkjet printing after 1, 3 and 7 days respectively. Bar = 200µm

3.4. NG108-15 neuronal ce ll phenotype after inkjet printing on days 1, 3 and 7

Neuronal cells are shown in figure 6. Samples were analysed according to standard methods (Daud et al. 2012).

Inkjet printed neuronal cells were found to have slightly longer neurites on average compared to control non-printed cells, and this difference was observed to increase over time until it became significant by day 7 (figure 7A). By day 3 neurites were becoming visibly longer compared to control, with an average of 65 µm versus 55 µm. By day 7, on average, inkjet printed cells had 0.25 more neurites, 12% more cells displayed neurites compared to controls and the longest neurites of inkjet printed cells were 20 µm longer.

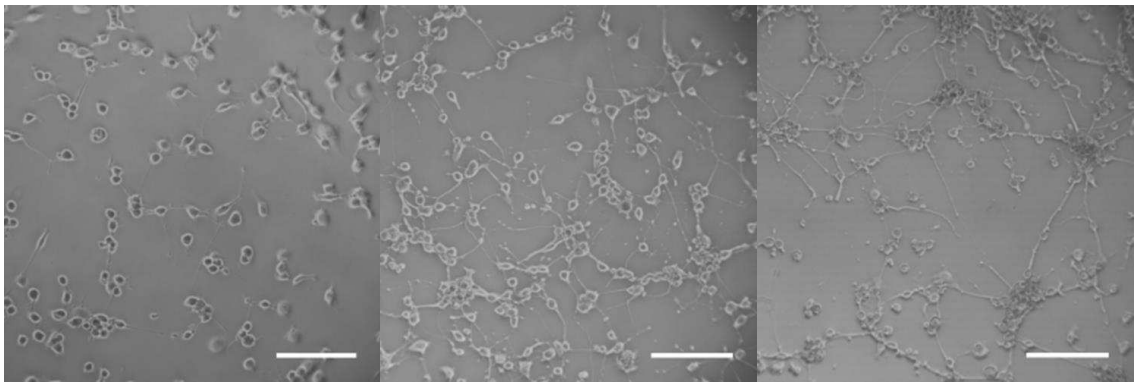

Fig. 6. Greyscale micrographs of NG108-15 cells after inkjet printing at 80V and 2kHz~~and ,~~ cultured without serum, after 1, 3 and 7 days respectively. Bar = 100µm

It was clear that not all neuronal cells produced neurites after serum starvation, even after 7 days. Over 85% of control cells expressed neurites versus 95% for ink-jet printed cells by day 7. While this difference was not significant, it was established that ink-jet printing, far from damaging neuronal cells, actually increased experimental differentiation. Figure 7B shows that neuronal cells more readily expressed neurites within the first day post printing compared to control. It is postulated that this is due either to a piezo electric effect, or results from a transient high shear stress during ejection through the small preface, or a combination of both. Figure 7C shows the average number of neurites was 1.7 and 1.1 per cell on day 1, to a maximum of 2.5 and 2.2 by day 7, for inkjet printed and control cells respectively (Figure 7C).

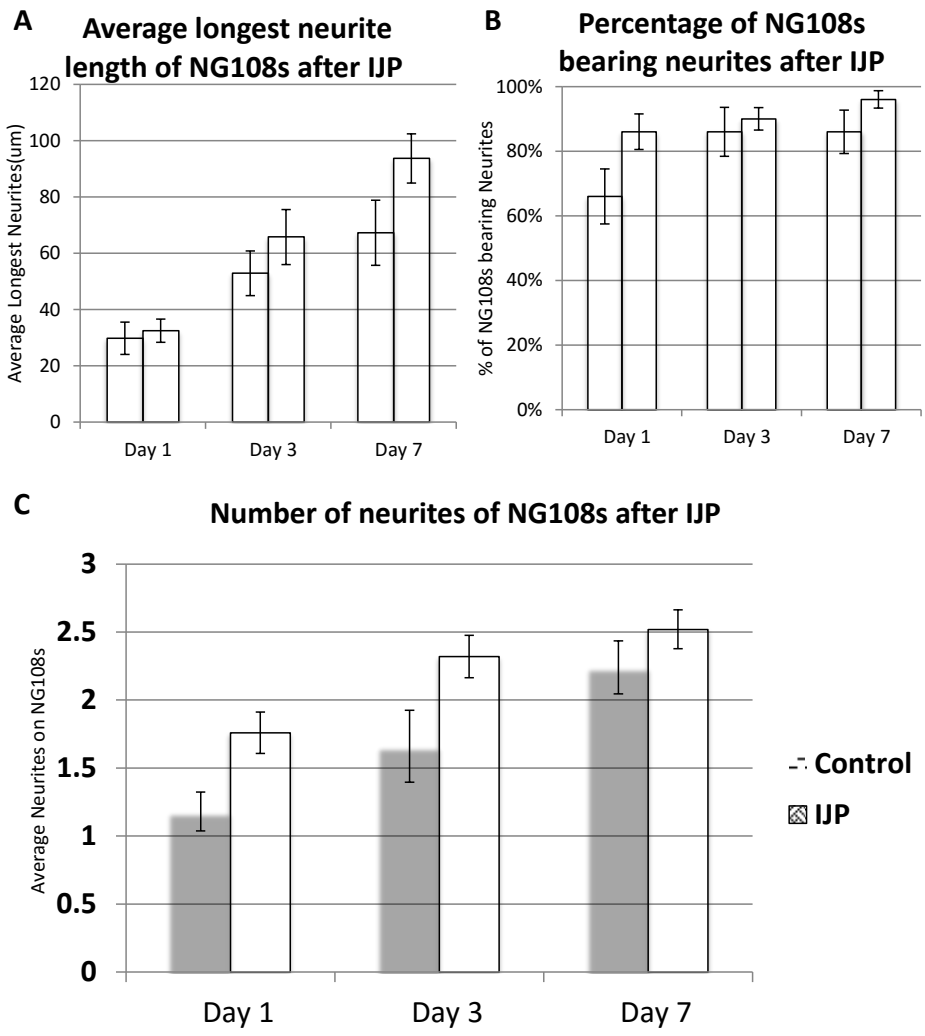


**Figure 7.** Quantitative measurements of NG108-15 cells that include standard deviation of average longest neurite length (A), percentage of cells bearing neurites (B) and number of neurites (C). Cells were cultured in serum-free cell medium to induce differentiation and the generation of neurites. Inkjet printed (IJP) cells were printed at 80V and a frequency of 2KHz. (n = 50).

Thus, piezoelectric printing caused neuronal cells to develop more neurites during the first 3 days after printing. By day 7, no other trends were observed that reached statistical significance, and the number of neurites were similar to controls, with the biggest difference being neurite length.
It is postulated that the inkjet printing process caused nerve cells to generate neurites earlier than normal and had longer neurites. This can be explained if it was assumed that the rate of growth of neurites is constant, and because more neurites were established by day 1 through the printing process, by day 7, the neurites from printed cells would be longer as they had longer to form. The implications of this study, showing inkjet printed cells generating more neurites initially post printing, could be of benefit to future research in cell-cell interactions, as inkjet printed nerves form more neurites initially (up to 3 days post printing, and then no statistical difference in number can be seen by day 7) and they have more time to extend and elongate compared to controls.

## 4. Conclusions

This study shows for the first time that NG108-15 neuronal cells and primary Schwann cells can be piezoelectrically printed with no adverse effects over a higher range of experimental voltages that have not been used previously. The process of piezoelectrically printing cells was not detrimental, as assessed immediately after printing and when assessed throughout 7 days following printing. The viability data for fibroblasts was comparable to that reported by Saunders (et al. 2008), who found a range of 94%-98% for piezoelectric voltages of 40V to 80V. In the present work this was extended to 230V - at this voltage fibroblasts had a viability of 89%, neuronal cells 96% and Schwann cells 90%, respectively. The higher voltages studied indicate better freedom of use of inkjet printing parameters can be used to create successful droplet formation for cell printing than previously investigated.
Schwann cells maintained their phenotype through the process of inkjet printing as shown by the presence of S100β, with data showing a slight increase in viability 7 days after printing compared to controls. Initial analysis showed more neurites were formed with inkjet printed cells, however by day 7, no statistical significance was seen. The initial increase in the number of neurites per cell with printed samples had an impact with neurite lengths, as they had more time to grow compared to controls. Printed neuronal NG108 cells displayed longer neurites than controls. Future work will focus

on printing co-cultures that will interact together to form biologically relevant in vitro tissue engineered constructs. Using inkjet printing to position neuronal cells could produce finer neuronal networks than previously produced, as printed cells produced longer neurites, with the implication that fewer cells may be required for a continuous neuronal system. The next stages will include the ability of printed networks to propagate action potentials, where such systems will be of benefit for advancing 3D in vitro lab chip devices and studies on neurodegenerative disorders.

## 5. References

Ahmed, Z. & Brown, R.A., 1999. Adhesion, alignment, and migration of cultured Schwann cells on ultrathin fibronectin fibres. Cell Motility and the Cytoskeleton, 42, pp.331–343.

Akassoglou, K. et al., 2002. Fibrin inhibits peripheral nerve remyelination by regulating Schwann cell differentiation. Neuron, 33, pp.861–875.

Baron-Van Evercooren, A. et al., 1982. Fibronectin promotes rat Schwann cell growth and motility. Journal of Cell Biology, 93, pp.211–216.

Boland, T. et al., 2003. Cell and organ printing 2: fusion of cell aggregates in three-dimensional gels. The anatomical record. Part A, Discoveries in molecular, cellular, and evolutionary biology, 272, pp.497–502.

Cui, S. et al., 2012. Direct Human Cartilage Repair Using Three-Dimensional Bioprinting Technology 1,2. Tissue engineering. Part A, 18, pp.1304–1313.

Cui, X. et al., 2010. Cell damage evaluation of thermal inkjet printed Chinese hamster ovary cells. Biotechnology and bioengineering, 106(6), pp.963–969.

Daud, M.F.B. et al., 2012. An aligned 3D neuronal-glial co-culture model for peripheral nerve studies. Biomaterials, 33, pp.5901–5913.

Discher, D.E., Janmey, P. & Wang, Y.-L., 2005. Tissue cells feel and respond to the stiffness of their substrate. Science (New York, N.Y.), 310, pp.1139–1143.

Ilkhanizadeh, S., Teixeira, A.I. & Hermanson, O., 2007. Inkjet printing of macromolecules on hydrogels to steer neural stem cell differentiation. Biomaterials, 28, pp.3936–3943.

Inamdar, N.K. & Borenstein, J.T., 2011. Microfluidic cell culture models for tissue engineering. Current Opinion in Biotechnology, 22, pp.681–689.

Kowtha, V.C. et al., 1993. Comparative electrophysiological properties of NG108-15 cells in serum-containing and serum-free media. Neuroscience letters, 164, pp.129–133.

Langer, R. & Vacanti, J.P., 1993. Tissue engineering. Science, 260, pp.920–926.

Lorber, B. et al., 2013. Adult rat retinal ganglion cells and glia can be printed by piezoelectric inkjet printing. Biofabrication, 6(1), p.015001.

Ma, W. et al., 2004. CNS stem and progenitor cell differentiation into functional neuronal circuits in three-dimensional collagen gels. Experimental neurology, 190, pp.276–288.

Miller, J.S. et al., 2012. Rapid casting of patterned vascular networks for perfusable engineered three-dimensional tissues. Nature Materials, 11, pp.768–774.

Parsa, S. et al., 2010. Effects of surfactant and gentle agitation on inkjet dispensing of living cells. Biofabrication, 2, p.025003.

Pepper, M.E. et al., 2011. Cell settling effects on a thermal inkjet bioprinter. 2011 Annual International Conference of the IEEE Engineering in Medicine and Biology Society, pp.3609–3612.

Phillippi, J. a et al., 2008. Microenvironments engineered by inkjet bioprinting spatially direct adult stem cells toward muscle- and bone-like subpopulations. Stem cells, 26(1), pp.127–134.

Saunders, R.E., Gough, J.E. & Derby, B., 2008a. Delivery of human fibroblast cells by piezoelectric drop-on-demand inkjet printing. Biomaterials, 29(2), pp.193–203.

Schwarz, U.S., Nelson, C.M. & Silberzan, P., 2014. Proteins, cells, and tissues in patterned environments. Soft matter, 10(14), pp.2337–40.

Tomba, C. et al., 2014. Tuning the adhesive geometry of neurons: length and polarity control. Soft matter, 10, pp.2381–7.

Wang, X., Yan, Y. & Zhang, R., 2007. Rapid prototyping as a tool for manufacturing bioartificial livers. Trends in biotechnology, 25(11), pp.505–13.

Wilson, W.C. & Boland, T., 2003. Cell and organ printing 1: protein and cell printers. The anatomical record. Part A, Discoveries in molecular, cellular, and evolutionary biology, 272, pp.491–496.

Xu, T., Zhao, W., Zhu, J.-M., Albanna, M.Z., et al., 2013. Complex heterogeneous tissue constructs containing multiple cell types prepared by inkjet printing technology. Biomaterials, 34(1), pp.130–9.

Xu, T. et al., 2005. Inkjet printing of viable mammalian cells. Biomaterials, 26, pp.93–99.

Zhang, Y. et al., 2012. Scaffolds for tissue engineering produced by inkjet printing. Central European Journal of Engineering, 2(3), pp.325–335.